ICARUS **126,** 126–137 (1997)
ARTICLE NO. IS965642

The Origin of the Moon and the Single Impact Hypothesis V[1]

A. G. W. CAMERON

Harvard–Smithsonian Center for Astrophysics, 60 Garden Street, Cambridge, MA 02138
E-mail: cameron@cfa.harvard.edu

Received May 29, 1996; revised October 17, 1996

Previous papers in this series have described the smooth particle hydrodynamics (SPH) method, which has been employed to explore the possibility that a major planetary collision may have been responsible for the formation of the Moon. In those simulations the SPH code used particles of equal mass and fixed smoothing lengths; I have found that the results obtained were reliable regarding what happens to the interiors of the colliding planets. Because the particles placed into the surrounding space were isolated rather than overlapping, however, that part of the calculation was unreliable. Ten additional cases have been run with 5000 particles in the Protoearth and 5000 in the Impactor, with variable smoothing lengths. Three of the cases had Protoearth/Impactor mass ratios of 5 : 5, 6 : 4, and 7 : 3. The other cases had a mass ratio of 8:2 and a variety of angular momenta. All cases had zero velocity at infinity. In every case the product of the collision became surrounded by evaporated particles of rock vapor, forming an extended atmosphere; however, relatively little mass extended beyond the Roche lobe. If the Moon formed from a rock disk in orbit around the Earth, then some other mechanism would be needed to transport angular momentum and mass outward in the equatorial plane, so that rock condensates from the hot atmosphere would be precipitated beyond the Roche limit, thus providing material for collection into the Moon. Most of this atmospheric material was originally in the Impactor and was mixed with terrestrial rock before evaporation. Recent calculations by R. M. Canup and L. W. Esposito (1996, *Icarus* 119, 427–446) have shown that it is very difficult to form the Moon from a gaseous disk largely confined to within the Roche lobe. On the other hand, higher-angular-momentum collisions can leave a quite massive body in orbit about the Earth, and this could form much or essentially all of the Moon. These questions remain challenging and require further investigations. © 1997 Academic Press

INTRODUCTION

The Giant Impact hypothesis was introduced two decades ago (Hartmann and Davis 1975, Cameron and Ward 1976). According to this hypothesis, toward the end of the planetary accumulation process, the Protoearth collided with a planetary body having a substantial fraction of the Protoearth mass. The collision took place with a fairly large impact parameter, so that the combined angular momentum of the two bodies was at least as great as that now in the Earth–Moon system. At the velocity characteristic of the collision (11–15 km/sec) most rocky materials are vaporized. Initially it was hypothesized that pressure gradients in the resulting vapor cloud played a crucial role in accelerating a relatively small fraction of the vapor into orbit about the Protoearth, forming a disk (Cameron and Ward 1976, Cameron 1985). The dissipation of this disk was then thought to spread matter radially so that the Moon could collect together gravitationally beyond the Roche lobe (Ward and Cameron 1978; Thompson and Stevenson 1983, 1988). The scenario has been reviewed by Stevenson (1987). We have subsequently found that gravitational torques are much more important than gas pressure gradients in planetary-scale collisions.

In a series of papers the author, with W. Benz and others [Paper I: Benz *et al.* (1986), Paper II: Benz *et al.* (1987), Paper III: Benz *et al.* (1989), Paper IV: Cameron and Benz (1991)], investigated this scenario through a number of simulations of the hypothetical Giant Impact. The tool used for the simulations was smooth particle hydrodynamics (SPH). In this method the domain of the computation is not divided into spatial cells, as in ordinary hydrodynamics, but rather the matter in the domain of computation is divided into smooth overlapping spheres. The density of a sphere has a radial distribution that is bell-shaped, with highest density at the center and a sharp outer edge. The particles carry individual internal energies, but such properties as density and presssure are collectively determined by the overlap between the density distributions of the particles; these are meaningful only when typically a few tens of particles contribute to the overlap.

In the above papers all particles were given the same mass (but could vary in composition), and their smoothing lengths were given fixed values. For purposes of maintaining comparability among the results, the original code was used for the later computations even though Willy

[1] Part V of a series. Part IV is Cameron and Benz (1991).

0019-1035/97 $25.00

Benz had developed versions that allowed variable masses and smoothing lengths. I now find that the results reported in Paper IV can be trusted to give good approximations to the dynamics of the collisions themselves and to the conditions in the interiors of the bodies in which extensive overlap of the particles occurred, but the particles in external orbits or that escaped were usually isolated from contact and thus could not respond to pressure gradients that would ordinarily affect their motions if they were in a gaseous state.

This was the reason why I initiated yet another series of simulations of the Giant Impact. In the earlier papers a total of 3008 particles were used for each simulation, all of the same mass. In the new simulations the total was raised to 10,000 particles, which were equally divided between the Protoearth and the Impactor, but in general the masses of the particles in these two bodies were unequal. The smoothing lengths of these particles were required to adjust so that a few tens of particles would overlap with any one of them. Thus, a particle isolated in space will stretch a long way to achieve this overlap. This made the determination of external atmospheres possible, although if few particles are present the atmospheric densities will be crudely approximated by this procedure.

In Paper IV the 41 reported runs were performed on a variety of low-end workstations; each typically took on the order of 6 weeks to complete. In the new series of runs the computations were carried out on somewhat higher performance workstations, most of them relatively inexpensive 486 machines. For these runs the bottleneck was not the speed of the CPU but the transfer of data from RAM to CPU, and thus different machines (including a UNIX machine) all ran the hydrocode at about the same rate within a total spread in time of less than a factor 2. The runs have typically taken about a year of continuous running time each. The runs used several different mass ratios of Impactor to Protoearth and varied the angular momentum in the collision. They were all started with zero velocity at infinity, and the results have been sufficiently definitive that it was clear that this parameter did not need to be varied. The previous series of simulations were carried out with both the Protoearth and the Impactor set to a temperature of 4000 K, presumed to have been developed by a prior history of collisions in the accumulations of these bodies. With the newer code, extensive evaporation of rock vapor would occur at this temperature, so the initial temperature was lowered to 2000 K to prevent this. The purpose of this assumption was to prevent rock evaporation from the planetary surfaces prior to collisions. The initial internal temperatures are underestimated by this assumption, but the present code does not support rigidity in solid materials, so the hydrodynamics are essentially unaffected by the lower temperature. The focus of this investigation is on the external matter in any case, so from that point of view it does not matter that the shock-induced internal temperatures may be slightly underestimated.

TABLE 1
Parameters of the Runs

Run	Angular momentum[a]	Mass ratio
AM02	2.216	5:5
AM03	1.965	4:6
AM04	1.666	3:7
AM05	1.213	2:8
AM06	1.433	2:8
AM09	1.576	2:8
AM10	1.647	2:8
AM08	1.719	2:8
AM07	1.990	2:8
AN01	0.000	2:8

[a] Angular momentum in units of the Earth–Moon system, 3.5×10^{41} cgs.

One run each was made with Protoearth-to-Impactor mass ratios of 5:5, 6:4, and 7:3, each with somewhat more than the angular momentum of the Earth–Moon system today. The remainder of the simulations were done for a ratio of 8:2 but with a variety of angular momenta in the collisions. One of the runs consisted of a central impact with zero angular momentum. These details are presented in Table I.

RESULTS

Figures 1 through 4 show snapshots of the progress of a Giant Impact from initial contact until the configuration has settled into nearly a final postimpact state. These figures show cases 2, 6, and 8 and the central impact, which represent a reasonable sampling of the types of phenomena observed. The major features of the simulations vary in a systematic way as the mass ratio changes at roughly a constant angular momentum, and these features also change systematically at the 8:2 ratio as the angular momentum is varied. The time durations in these figures lie in the range 1 to 2 days.

On the 486 machines the current state of the computation was normally displayed during the run as a color plot of the computational geometry. The internal energy of the particles was indicated to be within one of four energy ranges by the use of four different colors each for rock (dunite) and iron; I have found this to be much more useful for diagnostic purposes than using many colors in a pseudocontinuous distribution. In making these plots, the iron particles were plotted after the rock ones so that their images appeared superposed on the rock ones to see the behavior of iron within the planet without obscuration. This display scheme is also used in Figs. 1 through 4 for

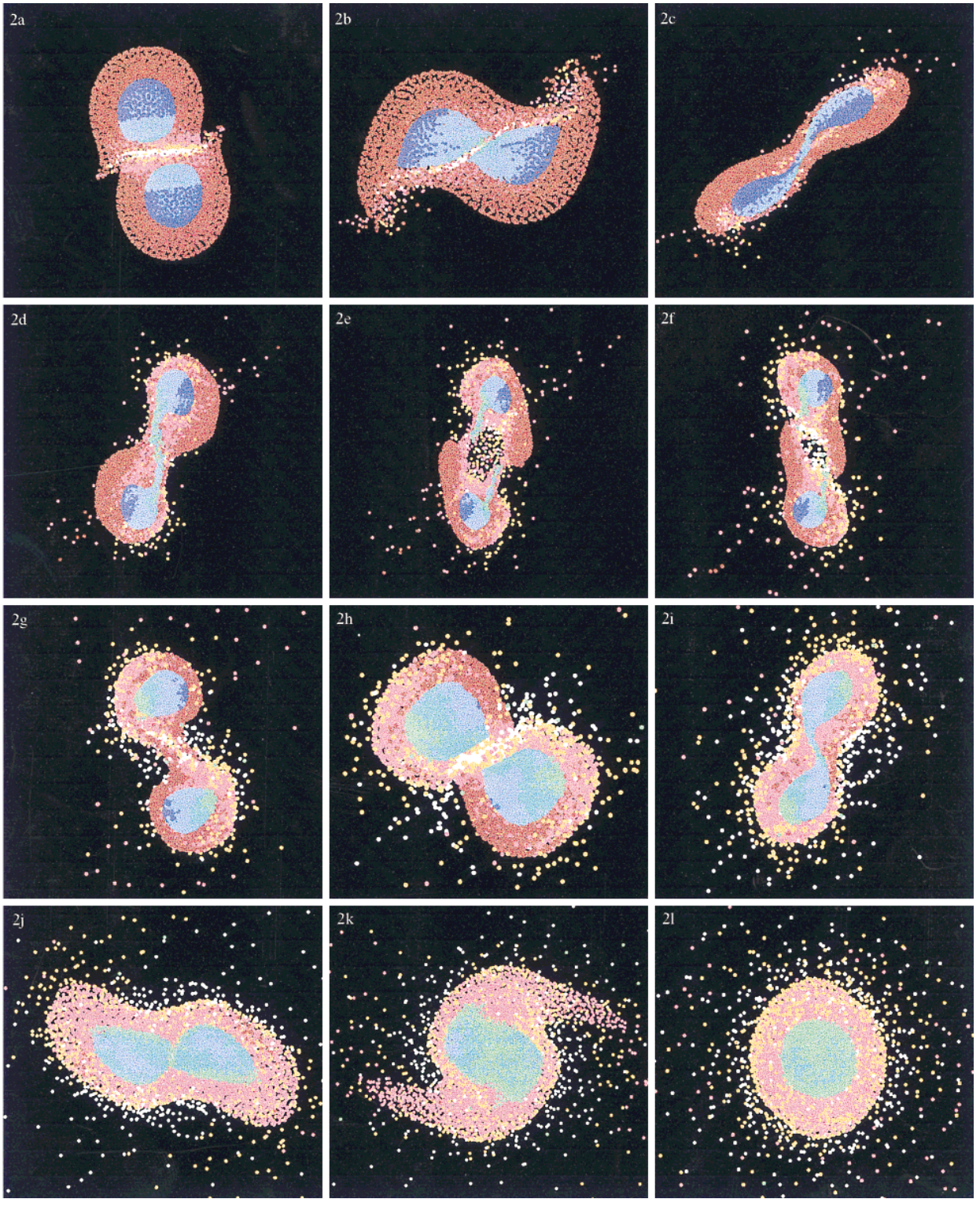

FIG. 1. Series of snapshots (panels 2a–2l) showing the progression of a Giant Impact between two equal masses each of $0.5M_{\oplus}$ (case 2). See the text for an explanation of the color coding. See also panel 2r in Fig. 2 for panel 2l rotated 90°.

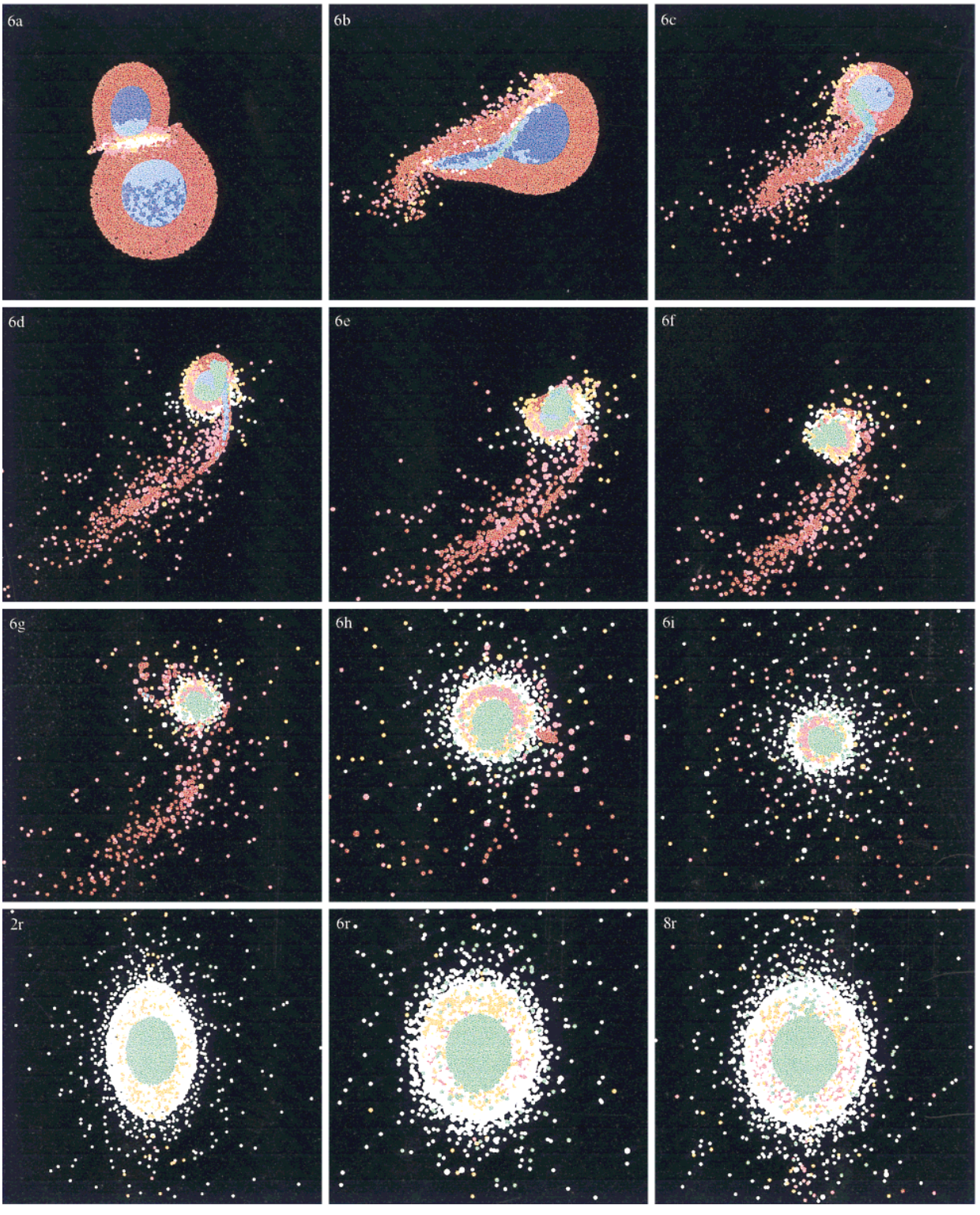

FIG. 2. Series of snapshots (panels 6a–6i) showing the progression of a Giant Impact between a Protoearth of $0.8M_{\oplus}$ and an Impactor of $0.2M_{\oplus}$ (case 6). The bottom row shows views of the final panels from Figs. 1–3 rotated 90°; these are designated 2r, 6r, and 8r.

the cases illustrated. For the dunite rock used to represent the mantle material the four colors used, in order of increasing internal energy, are dark red, light red or pink, brownish yellow, and white. The boundaries between these colors occurred at 1.24×10^{10}, 2.48×10^{10}, and 3.71×10^{10} erg/g. For iron used to represent the core material the colors used were dark blue, light blue, dark green, and light green in ascending order of internal energy. The boundaries between these colors occurred at 3.71×10^{10}, 7.42×10^{10}, and 1.12×10^{11} erg/g. These boundaries were empirically determined to provide a useful spread in the diagnostics over the range of conditions typically encountered in a Giant Impact. The higher values of the boundaries for iron reflect the fact that iron cores are typically heated to much higher temperatures than dunite mantle material in the course of the collisions.

Figure 1 (panels a–l) shows the collisional history of case 2, a symmetric collision between equal masses. The two bodies collide, as in panel 2a, form a very elongated configuration as in panel 2c, fall back together as in 2d, and then a hole opens up in the middle of the configuration as in 2e. The hole closes as the main parts of the two bodies collide again in the panels through 2h. In the remaining panels the iron cores merge into a central core surrounded by a very flattened oblate spheroid of rock. It is especially noticeable, starting at about panel 2g, that in regions where very hot rock is exposed on the surface, rock vapor particles (colored white) evaporate to form a small cloud of particles near such hot regions, and then these particles gradually spread around the entire planetary body. In the final panel, 2l, the postcollision body has become circular when viewed from the pole direction, as here, but is actually very rotationally flattened (as is shown in panel 2r of Fig. 2, which is the view of panel 2l rotated 90°). The white evaporated particles in the cloud surrounding the body are clustered most strongly toward the surface, as is characteristic of an atmosphere, and the density of white particles falls off away from the surface. Also visible at larger distances from the surface are many cooler (i.e., condensed) red particles shed at an earlier stage of the collision as seen in the panels up to 2g.

There is a characteristic outcome to all of the other asymmetric simulations. In the collision, the Impactor (i.e., the lower-mass body) becomes distorted and elongated; the bulk of it falls out into the Protoearth, including essentially all the central iron, which plunges right through the rock mantle of the Protoearth. The rock part of the Impactor farthest away from the point of impact has a general tendency to go into orbit about the Protoearth as individual particles (but sometimes as clumps of particles); however, the fallout of the iron core of the Impactor initially accumulates in a relatively small volume on one side of the Protoearth core, forming a rotating iron bar-like configuration inside the Protoearth. This can exert a powerful torque on clumps of particles outside the Protoearth, including in particular that part of the Impactor that would go into orbit but that is still largely contained in a relatively small volume. As the Impactor iron settles into the Protoearth core, the external rock material from the Impactor tends to be spread out into a trailing spiral wave (somewhat half of the configuration in panel 2k) and to move to larger radii. For the larger-mass ratios the behavior is essentially as depicted in Papers III and IV. The higher-angular-momentum cases often involve two collisions before the iron fallout goes to completion.

It was very striking to see, everywhere that a collision had heated the surface material of a planetary body, that a cloud of white particles arose above the surface and spread to surround the planetary body. Even greatly elongated configurations of the Impactor after the collision were surrounded by a cloud of white particles. For the 8 : 2 and 7 : 3 mass ratio cases the Impactor particles (of smaller mass) were plotted with smaller radii; from this it was possible to see that most of the particles (and a majority of the mass) in the white cloud were originally Impactor particles. Evidently when the planetary surface was heated by Impactor rock infall, the Impactor particles would tend to be on top of the Protoearth ones, and thus they would be first to evaporate. The white cloud was always densest next to the planetary surface and thinned out away from the surface, as would be expected for an atmosphere. This phenomenon was a major departure from that observed in the previous runs because the particle evaporation and formation of an atmosphere could not be properly simulated with fixed smoothing lengths and relatively few external particles.

The final states of the Protoearth following all of the collisions were remarkably similar. For this reason it is sufficient to show the results of four of the cases, runs 2, 6, and 8 and the central collision. These represent in case 2 a high-angular-momentum collision between two planets of half an Earth mass each, in cases 6 and 8 relatively low- and high-angular-momentum collisions between objects of 0.2 and 0.8 Earth mass, and in the central collision masses also of 0.2 and 0.8 Earth mass.

Figure 2 (panels 6a–6i) shows the results of a low-angular-momentum collision. Panel 6b shows the Impactor being destroyed through elongation. The side of the Impactor lying toward the center of the Protoearth is slowed in its motion by running into Protoearth material, whereas the other side encounters little such resistance and is slowed down much less. The iron core of the Impactor, being much denser, penetrates through most of the rock material and thus appears almost entirely on one side of the drawn-out debris, as may be seen in panel 6c. This iron core quickly falls back onto the Protoearth and penetrates through the rock mantle to pile up on one side of the Protoearth core (panel 6e). The rock that is left behind is distributed along

an arc extending away from the Protoearth, but lying on orbits that would bring it back to intersect the Protoearth surface if it were not for gravitational torques exerted by the nonspherical mass distribution of the Protoearth and the mass in its vicinity. It may be seen in panels 6d–6i that the Impactor iron has not had time to fully settle into the larger Protoearth core, and thus the mass distribution of the iron forms a rotating quadrupole, capable of exerting such gravitational torques. There is enough mass in the trailing rock arc to become gravitationally unstable and partially contract into a distinct clump of material, which can clearly be seen in panels 6d–6h until the clump impacts the surface in panel 6h. In the sequence of panels 6d–6i the evaporation of hot material from the Protoearth surface can be seen to be continuing; it has formed an extended atmosphere by panel 6i. Panel 6r in the middle of the bottom row of panels in Fig. 2 shows panel 6i rotated 90°. The rotational flattening is much less than in panel 2r, which is shown in the left position of the bottom row.

Figure 3 (panels 8a–8l) shows the results of a high-angular-momentum collision. Panel 8b shows the Impactor being stretched through a greater degree of elongation than in case 6. Panel 8c shows the elongated material beginning to gather itself together beyond the Roche lobe of the Protoearth. The iron core of the Impactor drifts toward the leading edge as before, but it does not immediately fall into the Protoearth. By panel 8d the bulk of the material in the Impactor has pulled itself together into a roughly spherical object, with the bulk of the iron core now again at the center (it may be seen in panel 8c that some of this Impactor core did fall into the Protoearth). In panel 8d the two planetary bodies are connected only by a thin line of material, and shortly afterward almost all of the remaining particles fall into one or the other planetary body. The reconstituted Impactor withdraws to a maximum distance of a few Protoearth diameters and then falls back to impact the Protoearth a second time in panel 8e. This time the Impactor is fully destroyed as in panels 8f and 8g, and as in case 6, the rock is drawn out into an arc while the iron falls into the Protoearth. Once again the Protoearth forms a rotating quadrupole. In panel 8j the rock arc has become very elongated and shows signs of instability. Two clumps form from this arc as may be seen in panel 8k; these have a fairly strong interaction. The closer clump gives up some of its angular momentum to the farther one and impacts the surface shortly after panel 8k. The final panel, 8l, shows the system some time later when the mass quadrupole has substantially subsided and the remaining clump has gone into a stable orbit that lies everywhere beyond the Roche lobe of the Protoearth. As in case 6, an extended atmosphere formed. This final panel, 8l, is shown rotated 90° in panel 8r at the right end of the bottom row of Fig. 2. It is not quite as rotationally flattened as in panel 2r.

The sequence shown in Fig. 3 is typical of the higher-angular-momentum cases that were run; in these cases two clumps resulted that behaved as shown in this figure. One of the clumps fell into the Protoearth and the other went into orbit. The surviving clump always had a mass much less than that of the Moon for the angular momentum range used in these cases.

The central impact case was run in part to study the formation of the impact-generated rock vapor atmosphere for a case uninfluenced by angular momentum. The case provided some rather spectacular examples of extreme deformation as a variety of modes of oscillation were induced in the Protoearth and as the resulting mechanical energy was gradually dissipated into heat. The sequence is shown in Fig. 4 (panels ca–cl). The impact occurs along the x axis (horizontal in the figure), and the large translational energy along this axis therefore excites modes with a predominance of x-axis deformation. When the Protoearth rebounds from such a deformation, the result is a symmetric deformation in the yz plane. Both the merged iron core and the rock mantle participate in the x-axis deformations, and the iron core itself has a small oscillation relative to the center of mass of the rock mantle. The damping of these motions is relatively rapid; the sequence of panels in the figure shows all of the major deformations that took place until the amplitude had greatly diminished. It may be seen that the iron core is quickly heated to high internal energy (light green in the figure), and the mantle is somewhat more slowly heated. At the end of the sequence the rock is roughly half-heated to the highest internal energy interval (white) and half to the next lower internal energy interval (yellow). The rock hemisphere farthest from the point of collisional impact (on the left) has clearly had more energy dissipated than the nearest hemisphere (on the right). Panels cc through ce clearly show that where the surface is hottest (white in the figure), the rate of particle evaporation is highest. By the end of the sequence an extended atmosphere had formed. What is not shown in this figure is that a significant number of the vaporized rock particles acquired a portion of the initial translational energy of the Impactor and formed a wind of rock vapor extending downstream in the direction of the impact. In most of the cases some of the particles escaped to infinity either as a wind (as in this case) or during the collision, but the amount of mass lost in this way was quite small.

Figure 5 shows the radial distribution of the particle temperatures for case 2, with iron plotted as black dots and rock as gray dots. Because of its different thermodynamic properties, iron becomes heated to much higher temperatures in a Giant Impact (I am indebted to H. J. Melosh for informing me that the highest temperature points for iron shown in this diagram are untrustworthy due to errors in the ANEOS data table for iron). It can be seen in Fig. 5 that the iron and rock are mixed up through much of

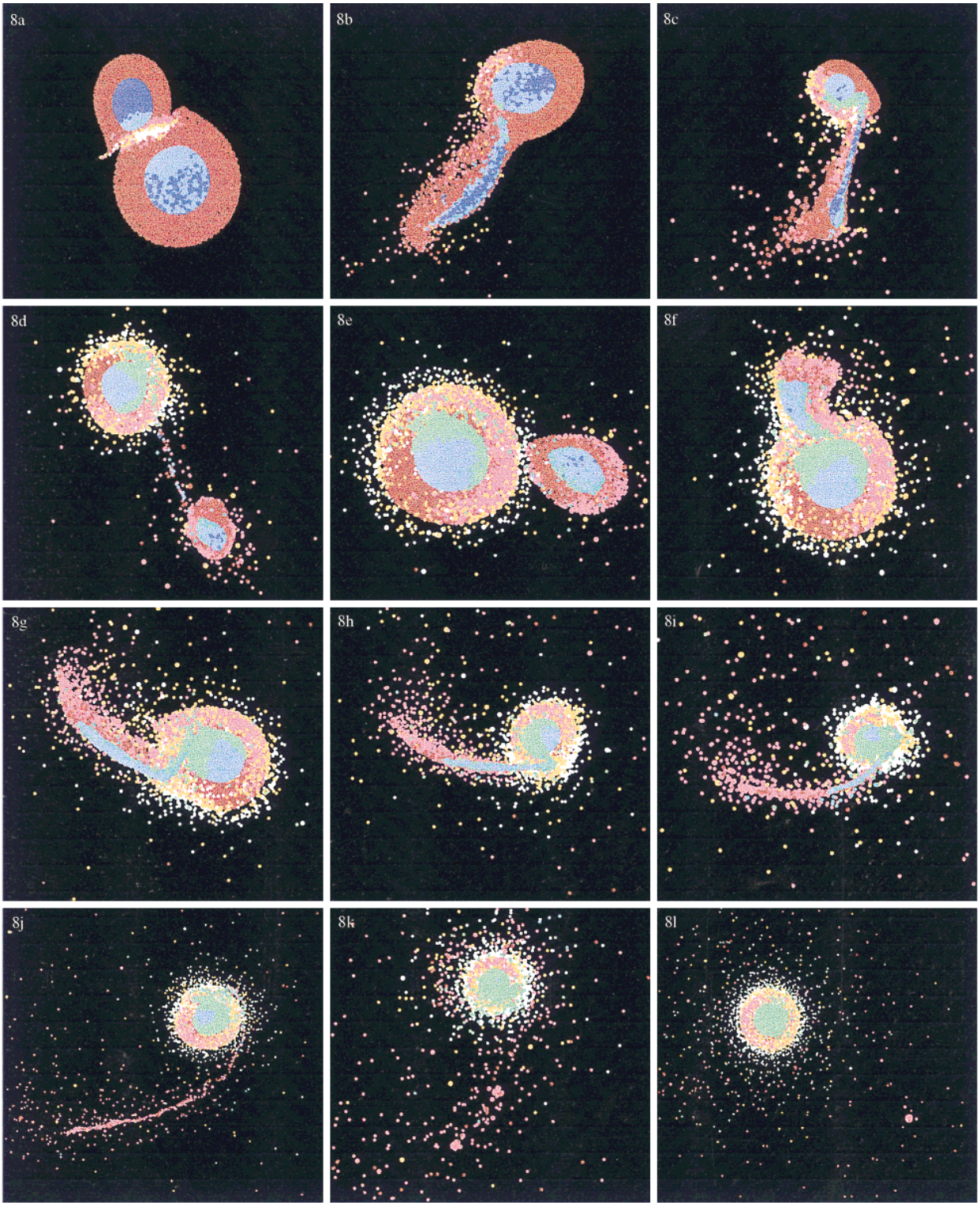

FIG. 3. Series of snapshots (panels 8a–8l) showing the progression of a Giant Impact between a Protoearth of $0.8M_{\oplus}$ and an Impactor of $0.2M_{\oplus}$ (case 8). See also panel 8r in Fig. 2 for panel 8l rotated 90°.

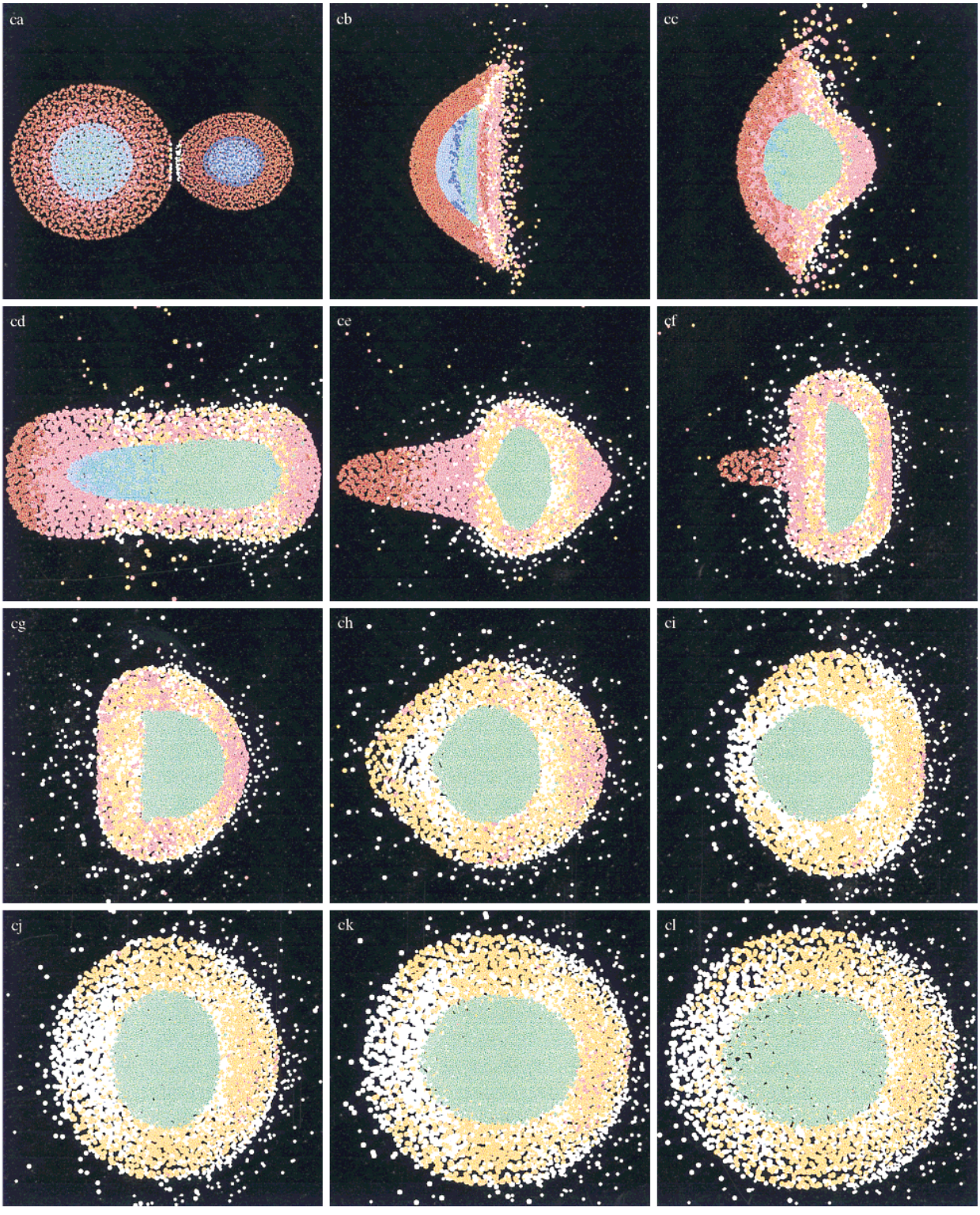

FIG. 4. Series of snapshots (panels ca–cl) showing the progression of a Giant Impact between a Protoearth of $0.8M_{\oplus}$ and an Impactor of $0.2M_{\oplus}$ (central impact case).

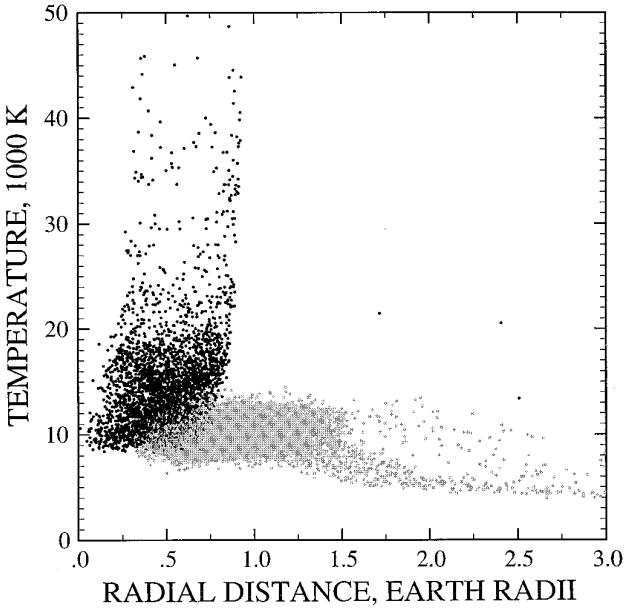

FIG. 5. Temperatures of the iron and dunite particles, as a function of radial distance, at the end of case 2. Iron particles are shown by black dots, dunite particles by gray dots. The base of the rock vapor atmosphere is at about 1.5 Earth radii.

the central region of the Protoearth. With time the rock will rise to sit on top of the iron, but with this merger of two equal masses, the dynamic readjustment was still in progress when the calculations were terminated. Note that the rock extends to a radial distance of about 1.5 Earth radii because of collisional heating and rotational flattening. Beyond 1.5 Earth radii the rock particles diminish in density in the region of the rock vapor atmosphere. The temperature of the rock particles remains high at larger distances because the higher entropy particles are bouyant in this atmosphere and thus tend to rise to greater heights, but this vertical sorting is also far from complete at the end of the computations.

Figure 6 shows the radial distribution of the particle temperatures for case 6. In this case the iron core of the Protoearth has been relatively little disturbed in the collision, but the iron core of the Impactor has fallen through a substantial gravitational potential in wrapping itself around the core of the Protoearth and, thus, has been much more extensively heated. Thus, the iron particles from the Impactor are fairly cleanly separated from, and at higher temperatures than, those of the Protoearth. Some of the iron particles from the Impactor are mixed in with rock particles in the mantle, and these will take longer to settle through the mantle (but these are also in the suspect thermodynamic regime according to Melosh).

In Figs. 5 and 6 it may be seen that an atmosphere of rock vapor particles extends above the surface of the mantle. These have a temperature of 4000 K or more and a very large scale height.

Figure 7 shows the radial variation of the density in the postcollision Protoearth out to a distance of 20 Earth radii, for cases 2 and 6 and also for the central collision. For cases 2 and 6 the atmospheric density has fallen by 11 orders of magnitude from that at the center of the Protoearth, and it has fallen even more for the central impact. The density at grid points on the equatorial plane was computed by summing the contributions from the overlapping particles; the distribution is very smooth because the particles at greater distances have correspondingly larger smoothing lengths. It must be cautioned that there are very few particles at these large distances, and hence the true atmospheric density must be distorted by the very large smoothing lengths; it will be too large at the greater radii because of the extent of the larger smoothing lengths for particles lower down. The density falls off more rapidly perpendicular to the equatorial plane. One can see a kink in the density distributions near 1.2 to 1.5 Earth radii, which we know from Figs. 5 and 6 to be the base of the atmosphere.

The temperature distributions for cases 2 and 6 are shown in more detail in Fig. 8. In this case the temperature of each particle contributing to a given grid point in the equatorial plane is weighted by the contribution of the particle density to that point, and the sum is then divided by the sum of the weights. The structure in the temperature variation at small distances arises from the interior of the Protoearth; the temperature varies smoothly outside of that. The average temperature stays above 4000 K out to

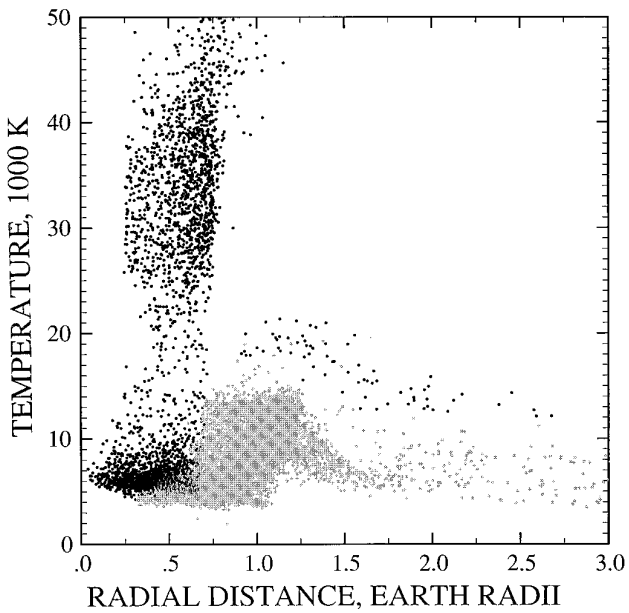

FIG. 6. Temperatures of the iron and dunite particles, as a function of radial distance, at the end of case 6. Iron particles are shown by black dots, dunite particles by gray dots. The base of the rock vapor atmosphere is at about 1.25 Earth radii.

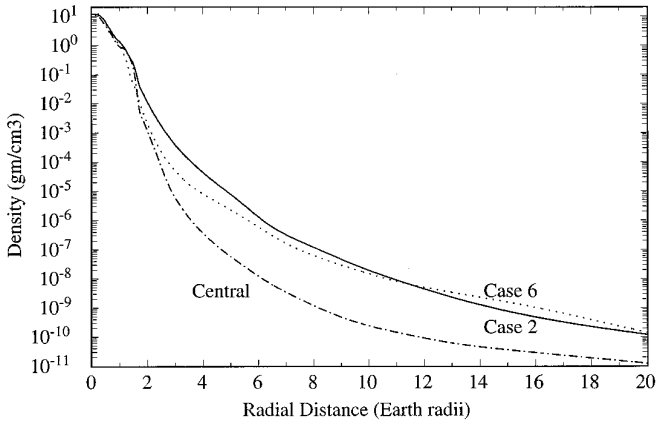

FIG. 7. Radial density variation of the rock vapor atmosphere in the equatorial plane of the Protoearth for cases 2 and 6 and the central impact.

about 8 Earth radii for both cases and slowly declines to larger distances for case 2, but not for case 6. This is also consistent with the bouyancy of higher-entropy material, but subject to distortion because of the larger smoothing lengths of the higher particles.

Figure 9 shows the radial variation of the specific angular momentum in the equatorial plane for cases 2 and 6. If the rock vapor atmosphere were in Keplerian rotation, the specific angular momentum would increase as the square root of the distance at larger distances. It may be seen that the rotation is sub-Keplerian in this sense.

This is confirmed by Fig. 10, which shows the angular velocity of the particles, averaged in the same way as the angular momentum, and for comparison the Keplerian angular velocity is also shown. The Keplerian values were computed for each particle by determining what the angular velocity would need to be to place that particle in circular Keplerian orbit. In this way the averaging of the contributions from each particle was done in the same way for the actual calculated angular velocity and the hypothetical Keplerian one. For each such particle's Keplerian angular velocity the effective central mass was taken to be the sum of the masses of all the particles at smaller distances from the center than that of the particle under consideration. It may be seen that in all cases the model angular velocity is significantly smaller than the Keplerian one. This indicates that at all distances the hydrostatic pressure gradient contributes a supporting force comparable to the centrifugal force at the same point.

DISCUSSION

Thus we arrive at a new and quite simple picture of the consequences of a Giant Impact. Wherever the surface of the Protoearth is hit hard by the impact, a very hot magma is produced. From this hot surface, rock vapor evaporates and forms a hot extended atmosphere around the Protoearth. The atmosphere is partly hydrostatically and partly centrifugally supported. The mean temperature is in excess of 4000 K out to about 8 Earth radii and is in excess of 2000 K out to about 20 Earth radii.

The above description would apply to just about any Giant Impact involving an Impactor with at least 10% of an Earth mass. A candidate Moon-forming Giant Impact must also possess at least the present value of the Earth–Moon angular momentum, which places constraints on the Impactor. Previous papers in this series have shown that the Impactor needs to have at least 14% of an Earth mass to swallow up the Impactor iron core and avoid getting too much iron in the Moon. But apart from this constraint it appears from the present simulations that any division of mass between the Protoearth and the Impactor can produce a promising set of conditions.

But how would the present set of similar scenarios evolve at subsequent times? Production and transport of radiation are not permitted by the code to occur in these models. The rationale for omitting them is that the time involved in the simulations is at most a day or two. In reality the scenarios would lead to cooling of the rock vapor atmosphere and precipitation of refractory materials at larger distances in the rock vapor atmosphere as it extends out into the equatorial plane. But the amount of mass in the atmosphere beyond the Roche limit (at 2.89 Earth radii) is far too little to form the Moon.

A scenario that might work under these conditions would be one in which most of the material in the Moon comes from that part of the Impactor that has been torqued into high Earth orbit, which requires a high-angular-momentum collision, such as in case 8. Several geochemists have told me of their dismay at the thought of having to accept such a scenario; however, as noted above, the

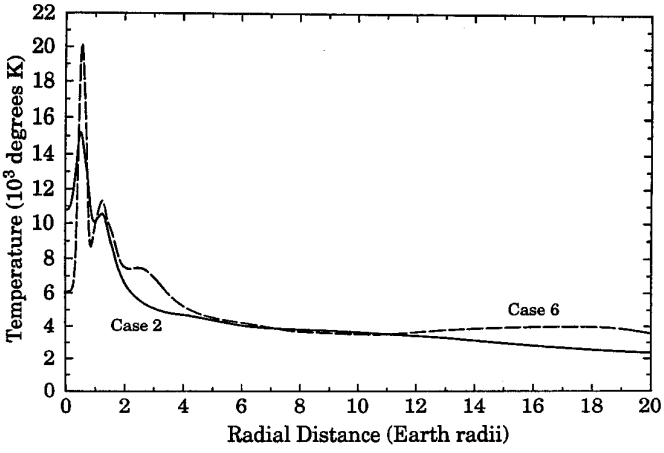

FIG. 8. Radial temperature variation of the rock vapor atmosphere in the equatorial plane of the Protoearth for cases 2 and 6.

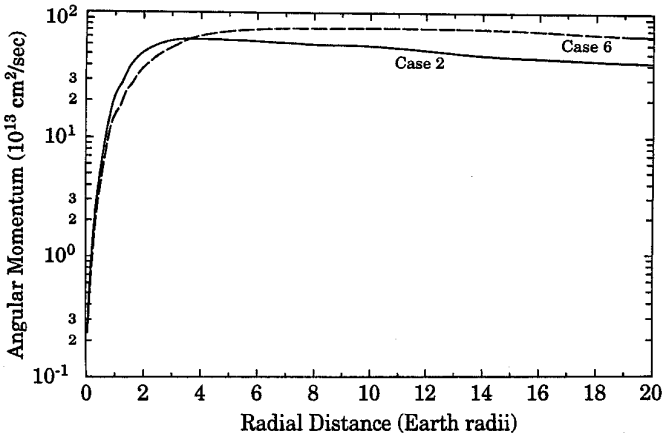

FIG. 9. Radial variation of the specific angular momentum in the rock vapor atmosphere in the equatorial plane of the Protoearth for cases 2 and 6.

satellites produced in the higher-angular-momentum collisions in the 8:2 mass ratio cases run here have too little mass to form a satisfactory Moon, even allowing for subsequent accretion. This suggests the desirability of simulating somewhat more symmetric collisions than 8:2 and higher-angular-momentum collisions, a combination of parameters that has not been explored. A major question for scenarios of this type is whether such a fragment of the impactor could lose enough volatile materials to resemble the composition of the Moon.

The problem of forming the Moon from a disk extending beyond the Roche limit has been analyzed in considerable detail by Canup and Esposito (1996). The required conditions turn out to be very constraining. The formation of a single lunar body requires that the many smaller bodies that might form out of the disk should decrease outward in mass, a condition that is contrary to their natural tendency unless the surface density of mass in the disk very steeply decreases outward. They find for this class of models that the total angular momentum in the collision must be about twice that in the current Earth–Moon system. This is not very different from many of the cases considered in the current set of runs. I find the results of this analysis to be very discouraging for those scenarios that involve relatively low-angular-momentum collisions, similar to case 6.

The angular momentum chosen for the runs in the current series was much higher than the value for the current Earth–Moon system. A motivation for this choice was to attempt to place material at larger distances from the Earth to promote lunar formation. But this raises the question of how the excess angular momentum is to be lost. One can postulate that a lot of mass was thrown out of the system at an early stage in the postcollisional evolution, but it is far from obvious how this might take place on a sufficient scale.

We know that angular momentum has been lost from the system as a result of solar tides on the Earth. The ratio of solar to lunar torque due to the ocean tide is 0.20, but if nonlinear friction in the oceans is taken into account, this increases to 0.29 (Munk and MacDonald 1975). Since lunar tides would have been relatively stronger in the early history of the Earth, it is most unlikely that more than a small part of the discrepancy can have been due to solar tides.

The Giant Impact, however, could have taken place when the Earth was only some 50 to 90% accumulated. If the Protoearth was only 50% accumulated, then the mass ratio of the Impactor to the Protoearth was still probably only around a third of the mass of the Protoearth, and the Giant Impact would be a scaled-down version of that illustrated in this paper, and the angular momentum would be similarly reduced. It remains to be seen how other aspects of the collision would scale. In this scenario one would look for the higher-angular-momentum cases in which a lunar-mass body is left in orbit but also leaving the system with roughly the present angular momentum.

If the Giant Impact took place when the Protoearth was 90% accumulated, then the last 10% of the mass to have been accumulated is likely to have included some very large bodies, perhaps including one of several percent of the Earth mass. For example, if the Impactor in the Giant Impact was a third of the mass of the Protoearth, then the second most massive object to be accumulated might have a mass about a third of that of the Impactor. This would be about 10% of an Earth mass. If this struck the Earth randomly after the Giant Impact, the angular momentum of the Earth–Moon system could have been very significantly modified.

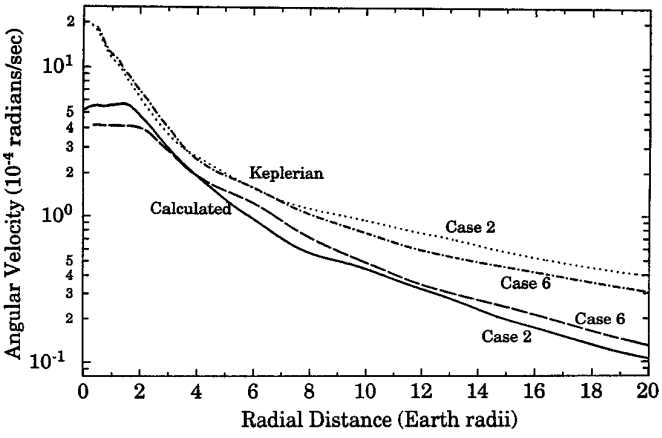

FIG. 10. Radial variation of the calculated angular velocity variation in the rock vapor atmosphere in the equatorial plane of the Protoearth for cases 2 and 6. Also shown is the Keplerian angular velocity required to place the atmosphere into Keplerian orbit about the Protoearth. This shows a partial hydrostatic pressure gradient support for the atmosphere.

The formation of the Moon as a postcollision consequence of a Giant Impact remains a hypothesis. The previous papers in this series appear to have characterized the internal effects of a Giant Impact on the Protoearth. The present paper has characterized the external environment of the Protoearth following a Giant Impact. The most promising direction for future simulations appears to involve Impactor/Protoearth mass ratios around 0.3 to 0.5 but a total mass at the time of the collision substantially less than a present Earth mass, and one would search for conditions in which a lunar-mass body is left in orbit after the collision.

ACKNOWLEDGMENTS

I thank Willy Benz for useful discussions. This work has been supported in part by NASA Grants NAGW-1598 from Planetary Materials and Geochemistry and NAGW-2277 from Origins of Solar Systems.

REFERENCES

Benz, W., W. L. Slattery, and A. G. W. Cameron 1986. The origin of the Moon and the single impact hypothesis I. *Icarus* **66,** 515–535. (Paper I)

Benz, W., W. L. Slattery, and A. G. W. Cameron 1987. The origin of the Moon and the single impact hypothesis II. *Icarus* **71,** 30–45. (Paper II)

Benz, W., A. G. W. Cameron, and H. J. Melosh 1989. The origin of the Moon and the single impact hypothesis III. *Icarus* **81,** 113–131. (Paper III)

Cameron, A. G. W. 1985. Formation of the prelunar accretion disk. *Icarus* **62,** 319–327.

Cameron, A. G. W., and W. Benz 1991. The origin of the Moon and the single impact hypothesis IV. *Icarus* **92,** 204–216. (Paper IV)

Cameron, A. G. W., and W. R. Ward 1976. The origin of the Moon. *Proc. Lunar Planet. Sci. Conf. 7th*, 120–122.

Canup, R. M., and L. W. Esposito 1996. Accretion of the Moon from an impact-generated disk. *Icarus* **119,** 427–446.

Hartmann, W. K., and D. R. Davis 1975. Satellite-sized planetesimals and lunar origin. *Icarus* **24,** 504–515.

Munk, W. H., and G. J. F. MacDonald 1975. *The Rotation of the Earth*. Cambridge Univ. Press, Cambridge, UK.

Stevenson, D. J. 1987. Origin of the Moon: The collision hypothesis. *Annu. Rev. Earth Planet. Sci.* **15,** 271–315.

Thompson, A. C., and D. J. Stevenson 1983. Two-phase gravitational instabilities in thin disks with application to the origin of the Moon. *Proc. Lunar Planet. Sci. Conf. 14th*, 787–788.

Thompson, A. C., and D. J. Stevenson 1988. Gravitational instability in two-phase disks and the origin of the Moon. *Astrophys. J.* **333,** 452–481.

Ward, W. R., and A. G. W. Cameron 1978. Disk evolution within the Roche limit. *Proc. Lunar Planet. Sci. Conf. 9th*, 1205–1207.